

# Vibrational Study of Phase Transitions in $\text{KIn}(\text{WO}_4)_2$

M. Mączka,<sup>\*,1</sup> J. Hanuza,<sup>\*</sup> S. Kojima,<sup>†</sup> and J. H. van der Maas<sup>‡</sup>

<sup>\*</sup>Institute for Low Temperature and Structure Research, Polish Academy of Sciences, P.O. Box 1410, 50-950 Wrocław 2, Poland; <sup>†</sup>Institute of Materials Science, University of Tsukuba, Tsukuba, Ibaraki 305-8573, Japan; and <sup>‡</sup>Department of Molecular Spectroscopy, University of Utrecht, Utrecht, the Netherlands

Received October 17, 2000; in revised form January 17, 2001; accepted February 9, 2001

**Studies of the low-temperature  $D_{2h}^{16}$  orthorhombic phase and investigation of trigonal–monoclinic phase transition in quenched high-temperature phase  $\text{KIn}(\text{WO}_4)_2$  were performed by means of infrared and Raman spectroscopy. The observed vibrational modes were assigned to the vibrations of respective atoms in the unit cells. It has been shown that as a result of the trigonal–monoclinic phase transition a similar temperature dependence of vibrational modes has been observed as that found for  $\text{KSc}(\text{WO}_4)_2$ , although crystallographic studies suggest that the former crystal has  $D_{3d}^4$  and the later  $D_{3d}^3$  structure.** © 2001

Academic Press

**Key Words:** double tungstates; vibrational spectra; phase transitions; ferroelastics.

## INTRODUCTION

$\text{KIn}(\text{WO}_4)_2$  belongs to the large family of crystals with the general formula  $M^I M^{III} (M^{VI} \text{O}_4)_2$ , where  $M^I$  = alkali metal ion,  $M^{III}$  = Al, In, Sc, Cr, Bi, Fe, rare-earth ion, and  $M^{VI}$  = Mo, W. These compounds have found application in quantum electronics (1–2). Many of them have been extensively studied because they exhibit interesting sequences of ferroelastic phase transitions from the paraelastic trigonal phase  $D_{3d}^3$  to monoclinic and triclinic phases (3–5). Recently, the existence of incommensurate phases was reported in a few crystals belonging to this family (6–8).

$\text{KIn}(\text{WO}_4)_2$  and  $\text{RbIn}(\text{MoO}_4)_2$  differ from the other crystals since they have two sequences of phase transitions. One sequence is realized in the rapidly quenched crystals having a trigonal structure near ambient temperature and the respective structural changes are similar to those for the other trigonal molybdates and tungstates. However,  $\text{KIn}(\text{WO}_4)_2$

<sup>1</sup>To whom correspondence should be addressed at Institute for Low Temperature and Structure Research, Polish Academy of Sciences, P.O. Box 1410, 50-950 Wrocław 2, Poland. Fax: 48 + 71-441029. E-mail: [maczka@int.pan.wroc.pl](mailto:maczka@int.pan.wroc.pl).

differs significantly from all the other crystals since its high-temperature structure is of  $D_{3d}^4$  symmetry (9), not  $D_{3d}^3$  as reported for other members of this family of layered compounds (except of  $\text{KFe}(\text{MoO}_4)_2$ ). The second sequence of phase transitions may be described as the transitions between the high-temperature trigonal  $D_{3d}^4$  (for  $\text{KIn}(\text{WO}_4)_2$ ) or  $D_{3d}^3$  (for  $\text{RbIn}(\text{MoO}_4)_2$ ) and the low-temperature  $D_{2h}^{16}$  phases. These transitions occur in slowly cooled crystals.

The present paper is devoted to studies of  $\text{KIn}(\text{WO}_4)_2$ . At first we are going to compare the results of IR and Raman investigation performed on orthorhombic crystals of  $\text{KIn}(\text{WO}_4)_2$  with our previous results obtained for  $\text{RbIn}(\text{MoO}_4)_2$  (10) in order to establish the origin of the observed bands. Then the temperature-dependent spectra measured for the trigonal crystals will be presented and analyzed. The aim of these investigations is to give some insight in the phase transition mechanism and to establish whether there are any noticeable differences in the vibrational properties of the  $D_{3d}^4$  and  $D_{3d}^3$  structures, and respective phase transitions into monoclinic or orthorhombic phases.

## EXPERIMENTAL

Single orthorhombic crystals were grown by the flux method developed by Klevtsov *et al.* (11) with a cooling rate 2 K/h and trigonal crystals with a cooling rate 10 K/min. The obtained needle-like orthorhombic and thin plate-like trigonal crystals were colorless. IR spectra were recorded with a Perkin Elmer 2000 FT-IR spectrometer. The polycrystalline spectra were measured in CsI suspension in the region 1100–150  $\text{cm}^{-1}$  and in nujol suspension in the region 600–30  $\text{cm}^{-1}$ . Raman spectra were recorded in the region 1100–200  $\text{cm}^{-1}$  with a Perkin Elmer 2000 FT-Raman spectrometer and the 1064 nm excitation. In the low-frequency region, below 200  $\text{cm}^{-1}$ , the Raman spectra were obtained with a triple-grating spectrometer of additive dispersion (Jobin Yvon, T64000) and 514.5 nm excitation. All spectra were recorded with a resolution of 2  $\text{cm}^{-1}$ .

**TABLE 1**  
Factor Group Analysis for the Trigonal Phase ( $D_{3d}^4$ ,  $Z = 2$ )

$D_{3d}$	$n(N)$	$n(T)$	$n(T')^a$	$n(L)$	$n(int)$	Activity	
						IR	Raman
$A_{1g}$	5	0	1	1	3	—	$xx + yy, zz$
$A_{2g}$	6	0	2	1	3	—	—
$E_g$	11	0	3	2	6	—	$xz, xx - yy, xy, yz$
$A_{1u}$	6	0	2	1	3	—	—
$A_{2u}$	7	1	2	1	3	$z$	—
$E_u$	13	1	4	2	6	$x, y$	—

<sup>a</sup>Raman active translational modes can be further subdivided into  $A_{2g} + E_g$  translational modes of  $K^+$  ions and  $A_{1g} + A_{2g} + 2E_g$  translational modes of  $WO_4^{2-}$  ions.

**TABLE 2**  
Factor Group Analysis for the Orthorhombic Phase ( $D_{2h}^{16}$ ,  $Z = 4$ )

$D_{2h}$	$n(N)$	$n(T)$	$n(T')$	$n(L)$	$n(int)$	Activity	
						IR	Raman
$A_{1g}$	22	0	8	2	12	—	$xx, yy, zz$
$B_{1g}$	22	0	8	2	12	—	$xy$
$B_{2g}$	14	0	4	4	6	—	$xz$
$B_{3g}$	14	0	4	4	6	—	$yz$
$A_u$	14	0	4	4	6	—	—
$B_{1u}$	14	1	3	4	6	$z$	—
$B_{2u}$	22	1	7	2	12	$y$	—
$B_{3u}$	22	1	7	2	12	$x$	—

## RESULTS AND DISCUSSION

### Low-Temperature Orthorhombic Phase

The crystal structure of the low-temperature modification of  $KIn(WO_4)_2$  obtained by the flux method is isostructural

to the orthorhombic  $D_{2h}^{16}$  structure of  $KIn(MoO_4)_2$  and the unit cell contains four molecular units (12). The tungstate tetrahedra occupy two nonequivalent sites in the orthorhombic crystal and as a result of the  $D_{3d}^4 \rightarrow D_{2h}^{16}$  phase transition the site symmetry is lowered from  $C_3$  to  $C_s$ . The

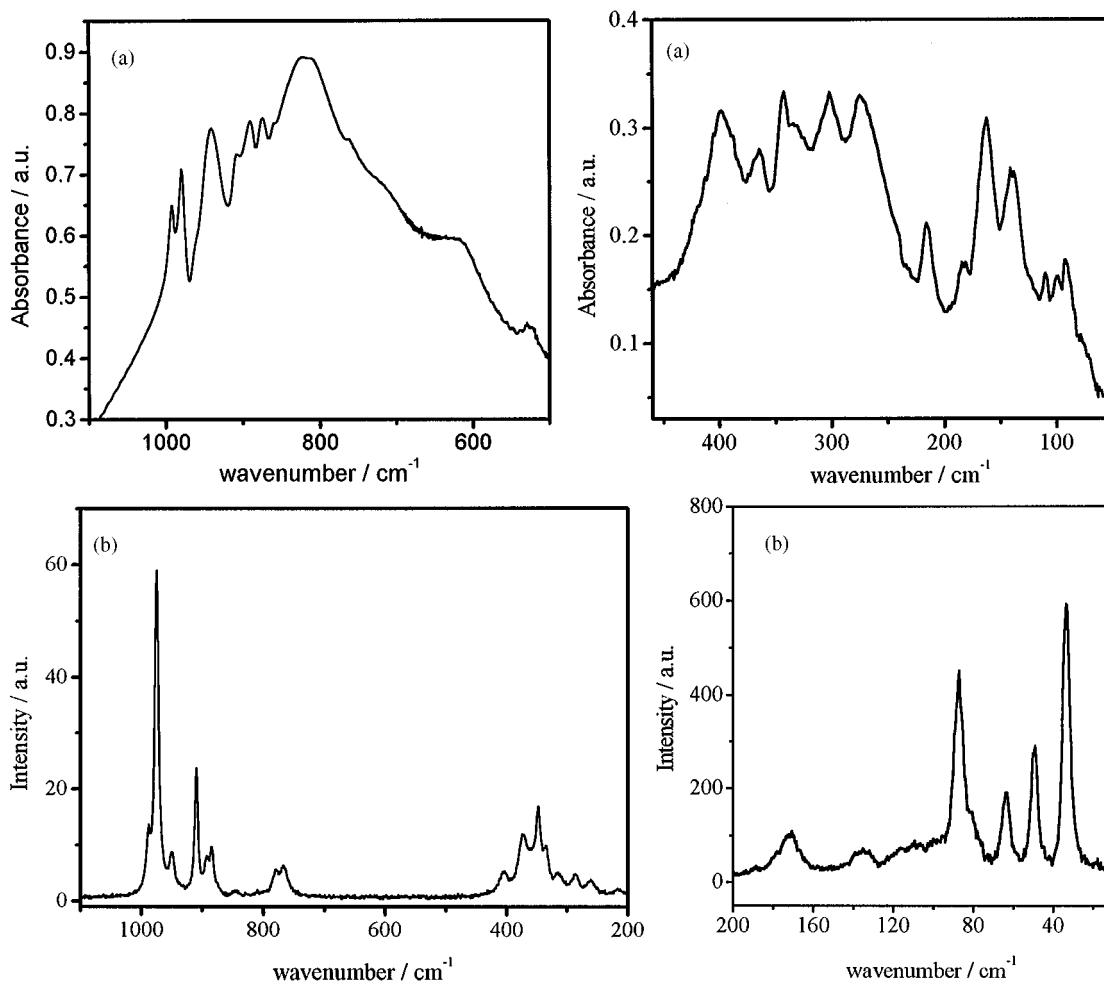


**FIG. 1.** Polycrystalline ambient temperature IR (a) and Raman (b) spectra of the orthorhombic phase of  $KIn(WO_4)_2$ .

results of factor group analysis for the both phases are shown in Tables 1 and 2 and the recorded IR and Raman spectra are presented in Fig. 1. The vibrational frequencies and the proposed assignment are shown in Table 3.

The vibrational spectra of  $\text{KIn}(\text{WO}_4)_2$  are very similar to the previously measured spectra of  $\text{RbIn}(\text{MoO}_4)_2$ . Since for the latter crystal the assignment of modes is known, the comparison of the results obtained for the both compounds allows us to propose assignment of the vibrational modes for  $\text{KIn}(\text{WO}_4)_2$  (see Table 3). This assignment shows a few differences between  $\text{RbIn}(\text{MoO}_4)_2$  and  $\text{KIn}(\text{WO}_4)_2$ . First,

all stretching modes for the tungstate ( $\nu_1 + \nu_3$ ) are shifted toward higher frequencies when compared to the molybdate. This shift is in agreement with the study of a number of molybdates and tungstates which showed that Mo–O stretching modes are generally located at lower frequency than W–O stretching modes in isostructural compounds (13). Second, the very weak and difficult to locate Raman-active mode observed at  $837 \text{ cm}^{-1}$  for  $\text{RbIn}(\text{MoO}_4)_2$  is now very clearly observed as a doublet at 885 and  $892 \text{ cm}^{-1}$ . Third, the IR spectra show the presence of some weak and broad bands in the range  $620\text{--}520 \text{ cm}^{-1}$  which were absent

**TABLE 3**  
Wavenumbers ( $\tilde{\nu}$ ) of the IR and Raman Modes for the Orthorhombic Phase of  $\text{KIn}(\text{WO}_4)_2$

RbIn(MoO <sub>4</sub> ) <sub>2</sub> ( $\tilde{\nu}/\text{cm}^{-1}$ )	IR KIn(WO <sub>4</sub> ) <sub>2</sub> ( $\tilde{\nu}/\text{cm}^{-1}$ )	Symmetry	RbIn(MoO <sub>4</sub> ) <sub>2</sub> ( $\tilde{\nu}/\text{cm}^{-1}$ )	Raman KIn(WO <sub>4</sub> ) <sub>2</sub> ( $\tilde{\nu}/\text{cm}^{-1}$ )	Symmetry	Assignment
986w	—	Depolarized	966w	—	Depolarized	Combination
967m	992m	<i>B</i> <sub>2u</sub>	961m	988w	<i>A</i> <sub>g</sub> + <i>B</i> <sub>1g</sub>	$\nu_1$
931m	980m	<i>B</i> <sub>2u</sub>	944vs	975vs	<i>A</i> <sub>g</sub> + <i>B</i> <sub>1g</sub>	$\nu_1$
956vw	960sh	<i>B</i> <sub>2u</sub>	950w	—	Depolarized	Combination
894m	940s	<i>B</i> <sub>2u</sub>	916m	949w	<i>A</i> <sub>g</sub> + <i>B</i> <sub>1g</sub>	$\nu_3$
860vw	908w	—	—	—	—	Combination
868m	890m	<i>B</i> <sub>2u</sub>	883m	910s	<i>A</i> <sub>g</sub> + <i>B</i> <sub>1g</sub>	$\nu_3$
834m	874m	<i>B</i> <sub>2u</sub>	837vw	892w	<i>A</i> <sub>g</sub> or <i>B</i> <sub>1g</sub>	$\nu_3$
—	—	—	—	885m	<i>A</i> <sub>g</sub> or <i>B</i> <sub>1g</sub>	$\nu_3$
—	859sh	—	—	—	—	Combination
802m	822vs	<i>B</i> <sub>2u</sub>	773m	779m	<i>A</i> <sub>g</sub> + <i>B</i> <sub>1g</sub>	$\nu_3$
791vs	810vs	<i>B</i> <sub>1u</sub>	800m	845m	<i>B</i> <sub>2g</sub> + <i>B</i> <sub>3g</sub>	$\nu_3$
745w	762w	<i>B</i> <sub>1u</sub>	748m	764m	<i>B</i> <sub>2g</sub> + <i>B</i> <sub>3g</sub>	$\nu_3$
—	618w,b	—	—	—	—	W–O ... W
—	525w,b	—	—	—	—	W–O ... W
402s	398s	—	397w	405m	<i>A</i> <sub>g</sub> + <i>B</i> <sub>1g</sub>	} $\nu_2 + \nu_4$
373s	355w	—	370m	373s	<i>A</i> <sub>g</sub> + <i>B</i> <sub>1g</sub> + <i>B</i> <sub>2g</sub> + <i>B</i> <sub>3g</sub>	
343m	344s	—	344w	348s	<i>B</i> <sub>2g</sub> + <i>B</i> <sub>3g</sub>	
327w	333sh	—	330m	336w	<i>A</i> <sub>g</sub> + <i>B</i> <sub>1g</sub>	
307w	302s	—	318m	316w	<i>B</i> <sub>2g</sub> + <i>B</i> <sub>3g</sub>	
281s	—	—	300w	287w	<i>A</i> <sub>g</sub> + <i>B</i> <sub>1g</sub>	
266s	275s	—	262w	261w	<i>A</i> <sub>g</sub> + <i>B</i> <sub>1g</sub> + <i>B</i> <sub>2g</sub> + <i>B</i> <sub>3g</sub>	
219m	215w	—	222w	218w	<i>A</i> <sub>g</sub> + <i>B</i> <sub>1g</sub>	
204w	202vw	—	217w	—	<i>B</i> <sub>2g</sub> + <i>B</i> <sub>3g</sub>	
—	181sh	—	166w	172m	<i>A</i> <sub>g</sub> + <i>B</i> <sub>1g</sub>	
178m	164s	—	163w	—	<i>B</i> <sub>2g</sub> + <i>B</i> <sub>3g</sub>	} <i>T'</i> ( <i>MO</i> <sub>4</sub> ), <i>T'</i> ( <i>M</i> <sup>+</sup> ) and <i>T'</i> ( <i>MO</i> <sub>4</sub> ) * <i>T'</i> ( <i>In</i> <sup>3+</sup> )
162s	143m	—	146w	135m	<i>A</i> <sub>g</sub> + <i>B</i> <sub>1g</sub>	
140m	138m	—	124w	—	—	
—	—	—	105sh	107w	<i>B</i> <sub>2g</sub> + <i>B</i> <sub>3g</sub>	
—	—	—	99sh	100vw	—	} <i>L</i> ( <i>MO</i> <sub>4</sub> )
—	—	—	93w	—	<i>B</i> <sub>2g</sub> + <i>B</i> <sub>3g</sub>	
104vw	—	—	110m	88s	<i>A</i> <sub>g</sub> + <i>B</i> <sub>1g</sub>	
90m	111w	—	—	—	—	
81w	101w	—	—	—	—	
74m	90w	—	77m	65s	<i>A</i> <sub>g</sub> + <i>B</i> <sub>1g</sub> + <i>B</i> <sub>2g</sub> + <i>B</i> <sub>3g</sub>	
68vw	71w	—	—	—	—	
62vw	—	—	61s	—	<i>A</i> <sub>g</sub> + <i>B</i> <sub>1g</sub>	
51vw	—	—	54m	50m	<i>A</i> <sub>g</sub> + <i>B</i> <sub>1g</sub>	
44vw	—	—	41m	34s	<i>A</i> <sub>g</sub> + <i>B</i> <sub>1g</sub> + <i>B</i> <sub>2g</sub> + <i>B</i> <sub>3g</sub>	

Note. The assignment of vibrational modes is based on comparison with the previously published spectra of  $\text{RbIn}(\text{MoO}_4)_2$  (10). vs, s, m, w, vw, and b denote very strong, strong, medium, weak, very weak, and broad, respectively. *MO*<sub>4</sub> denotes  $\text{WO}_4^{2-}$  or  $\text{MoO}_4^{2-}$  and *M*<sup>+</sup> denotes  $\text{K}^+$  or  $\text{Rb}^+$ .

for  $\text{RbIn}(\text{MoO}_4)_2$ . Such broad bands appear usually as a result of intermolecular interactions between molybdate or tungstate tetrahedra, which lead to formation of  $\text{W-O}\cdots\text{W}$  oxygen bridges. Therefore, the present results may indicate that the  $\text{WO}_4^{2-}$  tetrahedra are not well isolated. It is worth mentioning that this conclusion is consistent with the results of low-temperature synthesis (at  $550^\circ\text{C}$ ), which shows that  $\text{KIn}(\text{WO}_4)_2$  may be obtained in the structure similar to that of  $\alpha\text{-KY}(\text{WO}_4)_2$  (14). In this structure  $\text{WO}_4$  tetrahedra are connected through the  $\text{W-O}\cdots\text{W}$  oxygen bridges and when crystals are heated they transform at  $730^\circ\text{C}$  into the orthorhombic  $D_{2h}^{16}$  structure. Fourth, in the lattice modes region (i.e., below  $300\text{ cm}^{-1}$ ) majority of bands exhibit downward frequency shift when Mo atoms are replaced by W atoms. However, this shift is relatively small (less than  $22\text{ cm}^{-1}$ ). Such a result indicates that the lattice modes are strongly coupled. In summary, the vibrational characteristics of the low-temperature phases of  $\text{RbIn}(\text{MoO}_4)_2$  and  $\text{KIn}(\text{WO}_4)_2$  is very similar, in agreement with the X-ray data suggesting that these phases are isostructural.

#### Temperature Dependence of Vibrational Spectra for the High-Temperature Trigonal Phase of $\text{KIn}(\text{WO}_4)_2$

We may expect to observe significant differences in vibrational properties and phase transition mechanisms for  $\text{KIn}(\text{WO}_4)_2$  and  $\text{KSc}(\text{WO}_4)_2$ , since the paraelastic phases of these compounds have different symmetries and contain

different number of formulas in the unit cell. The main consequences of different space groups are as follows:

— The number of vibrational modes is doubled for the  $D_{3d}^4$  structure (see factor group analysis presented in Table 1 and Ref. 15). Since, however,  $A_{2g}$  and  $A_{1u}$  modes are IR and Raman inactive we expect to observed the same number of nondegenerate internal modes for both  $D_{3d}^3$  and  $D_{3d}^4$  structures, whereas the doubling is expected for the degenerate modes of the  $D_{3d}^4$  structure.

— Only one librational mode ( $E_g$ ) is expected to be Raman active for the  $D_{3d}^3$  structure (see Ref. 15), but in case of the  $D_{3d}^4$  symmetry this mode should split into two  $E_g$  components. Additionally, the  $A_{2g}$  librational mode inactive for the  $D_{3d}^3$  structure should be observed for the  $D_{3d}^4$  structure, since it should split into  $A_{1g} + A_{2g}$  components.

— No translational modes of  $\text{K}^+$  ions ( $T'(\text{K}^+)$ ) are Raman active for the  $D_{3d}^3$  structure, whereas one  $T'(\text{K}^+)$  mode of  $E_g$  symmetry should be observed for the  $D_{3d}^4$  structure. One should notice, however, that this  $E_g$  mode describes the out-of-phase motions of  $\text{K}^+$  ions in the adjacent unit-cells along the threefold axis. Our former studies of  $\text{KSc}(\text{WO}_4)_2$  showed that such a vibration is most likely responsible for the phase transition and it is observed as two soft modes below the phase transition temperature ( $T_1$ ) due to the folding of the Brillouin zone (BZ) boundary soft mode into the BZ center (15). In case of the  $D_{3d}^4$  structure, however, the  $c$ -period is already doubled in comparison with the  $D_{3d}^3$  structure and therefore no doubling occurs due to the phase transition. This means that the  $D_{3d}^4 \rightarrow C_{2h}^6$  transition is

TABLE 4  
Wavenumbers ( $\tilde{\nu}$ ) of the IR and Raman Modes for the Trigonal (at 490 K) and Monoclinic (at 293 K) Phases of  $\text{KIn}(\text{WO}_4)_2$

IR			Raman						
$\text{RbIn}(\text{MoO}_4)_2$ 293 K ( $\tilde{\nu}/\text{cm}^{-1}$ )	$\text{KIn}(\text{WO}_4)_2$ 490 K ( $\tilde{\nu}/\text{cm}^{-1}$ )	Symmetry	$\text{KIn}(\text{WO}_4)_2$ 293 K ( $\tilde{\nu}/\text{cm}^{-1}$ )	$\text{KSc}(\text{WO}_4)_2$ 293 K ( $\tilde{\nu}/\text{cm}^{-1}$ )	$\text{KIn}(\text{WO}_4)_2$ 490 K ( $\tilde{\nu}/\text{cm}^{-1}$ )	Symmetry	$\text{KSc}(\text{WO}_4)_2$ 100 K ( $\tilde{\nu}/\text{cm}^{-1}$ )	$\text{KIn}(\text{WO}_4)_2$ 293 K ( $\tilde{\nu}/\text{cm}^{-1}$ )	Assignment
963sh	992sh	$A_{2u}$	1001w + 998w	1011s	1005s	$A_{1g}$	1012s	1006s	$\nu_1$
—	—	—	—	—	—	—	—	950w	$\nu_3$
929w	914sh	$A_{2u}$	924w + 919w	928m	928s	$A_{1g}$	927m	928s	$\nu_3$
846s	851vs	$E_u$	859s + 830s	808m	801m	$E_g$	817m + 806m	811m + 790m	$\nu_3$
—	358sh	$A_{2u}$	381w	360w	353w	$A_{1g}$	372w	362m	$\nu_4$
346m	333w	$E_u$	332m + 341sh	345s	338s	$E_g$	345s + 352m	339sh + 333s	$\nu_2$
296m	301s	$E_u$	301s	327w	320w	$E_g$	332m	321m	$\nu_4$
200s	190s	$E_u$	194s	—	—	—	—	—	$T'(\text{In}^{3+})^*T'(MO_4)$
—	—	—	162w	140m	139m	$E_g + A_{1g}$	136m + 147m	143m	$T'(MO_4)$
—	—	—	146w	—	—	—	—	112w	$T'(M^+)$
—	—	—	—	—	—	—	103w	91w	$L(MO_4)$
117m	—	$E_u$	124sh	60m	—	$E_g$	59w	58w	$L(MO_4)$
60vw	—	—	103w	—	—	—	37w	49w	Soft mode
—	—	—	—	—	—	—	16w	34w	Soft mode

Note. The assignment is based on comparison with the previously published spectra of  $\text{KSc}(\text{WO}_4)_2$  and  $\text{RbIn}(\text{MoO}_4)_2$  (10, 15). Symmetry is given for the trigonal phases of  $\text{RbIn}(\text{MoO}_4)_2$  (at 293 K),  $\text{KIn}(\text{WO}_4)_2$  (at 490 K), and  $\text{KSc}(\text{WO}_4)_2$  (at 293 K).  $MO_4$  denotes  $\text{MoO}_4^{2-}$  or  $\text{WO}_4^{2-}$  and  $M^+$  denotes  $\text{K}^+$  or  $\text{Rb}^+$ .

due to an instability of a BZ center soft mode, which should be active in the both phases.

The measured Raman spectra are very similar to the spectra of other double molybdates and tungstates (10,15,16) and therefore the assignment of majority of bands is straightforward (see Table 4 and Figs. 2 and 3). This similarity is due to the fact that the Raman spectra give information about internal and lattice modes of  $\text{WO}_4^{2-}$  and  $\text{MoO}_4^{2-}$  ions only. In case of IR spectra the situation is more complicated since the translations of alkali-metal and trivalent ions are IR active. Having in mind that the frequencies of the translational modes of alkali-metal and trivalent ions should depend strongly on the respective atomic mass, we assigned the measured bands comparing the spectra with the spectra obtained for other double molybdates and tungstates (see Table 4). It is worth noticing that the dependence on the type of a trivalent ion is observed even for the doubly degenerate stretching modes, although these modes are well separated from the lattice

modes. Our measurements show that whereas the  $E_g$  stretching modes are observed in the narrow frequency range for  $\text{KAl}(\text{MoO}_4)_2$ ,  $\text{KIn}(\text{WO}_4)_2$ , and  $\text{KSc}(\text{WO}_4)_2$  (i.e.,  $800\text{--}807\text{ cm}^{-1}$  (15,16)), the respective  $E_u$  modes are observed for these compounds at  $880$ ,  $851$ , and  $819\text{ cm}^{-1}$  (17,18). Such pronounced differences between the  $E_g$  and  $E_u$  modes indicate the large contribution of long-range Coulomb forces to the  $E_u$  modes.

We cannot observe any splitting of the  $E_g$  modes into doublets, as expected for the  $D_{3d}^4$  structure. This may be due to the fact that the  $D_{3d}^4$  structure is very similar to the  $D_{3d}^3$  one and it differs, according to Ref. 9, only in slight distortion of oxygen arrangement pattern. Raman measurements at  $490\text{ K}$  show the presence of only one lattice mode at  $139\text{ cm}^{-1}$ . This mode can be assigned to the translations of  $\text{WO}_4^{2-}$  tetrahedra ( $T'(\text{WO}_4)$ ). These two overlapping modes of  $A_{1g}$  and  $E_g$  symmetry were observed at  $140\text{ cm}^{-1}$  for  $\text{KSc}(\text{WO}_4)_2$  (15). We cannot observe at  $490\text{ K}$  any bands, which could be assigned to librational and Raman active

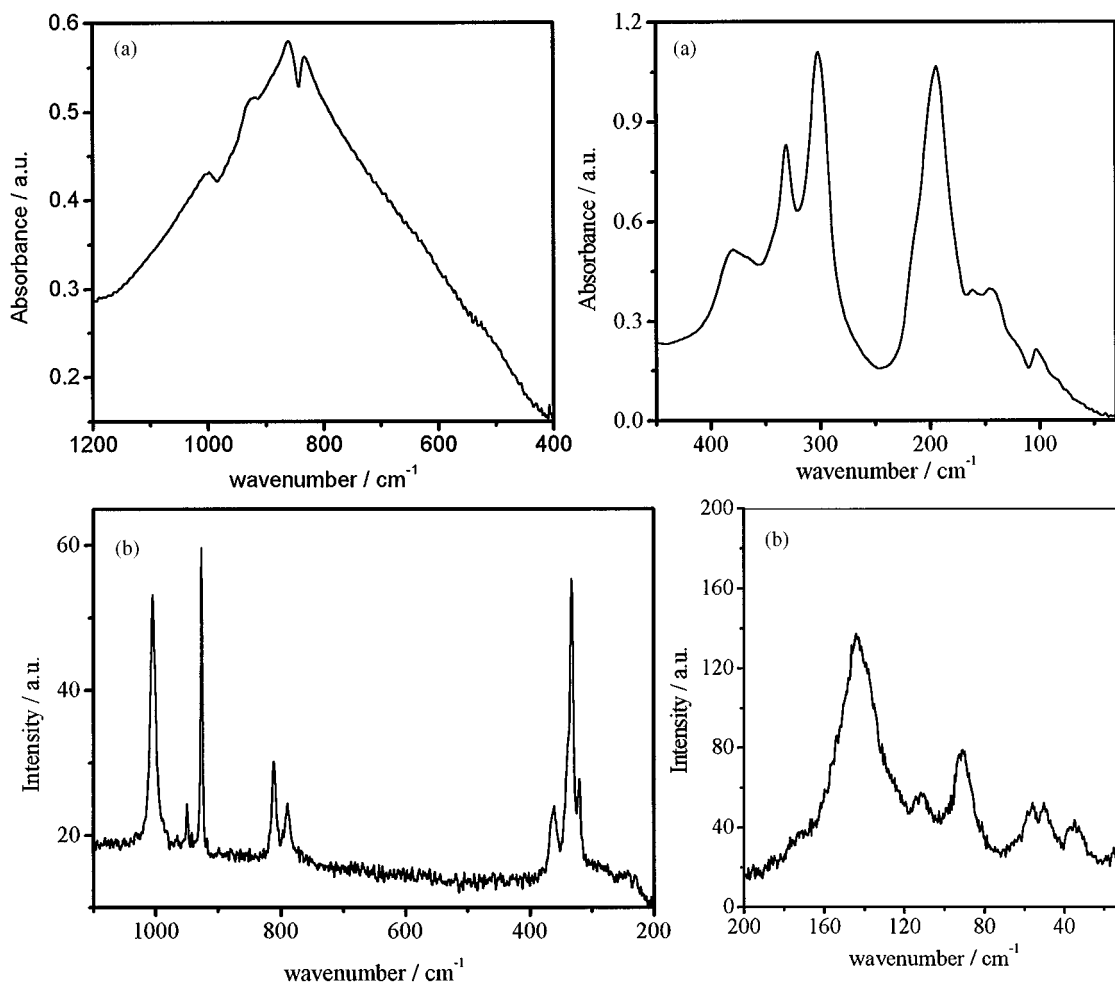


FIG. 2. Polycrystalline ambient temperature IR (a) and Raman (b) spectra of the pseudo-trigonal (monoclinic) phase of  $\text{KIn}(\text{WO}_4)_2$ .

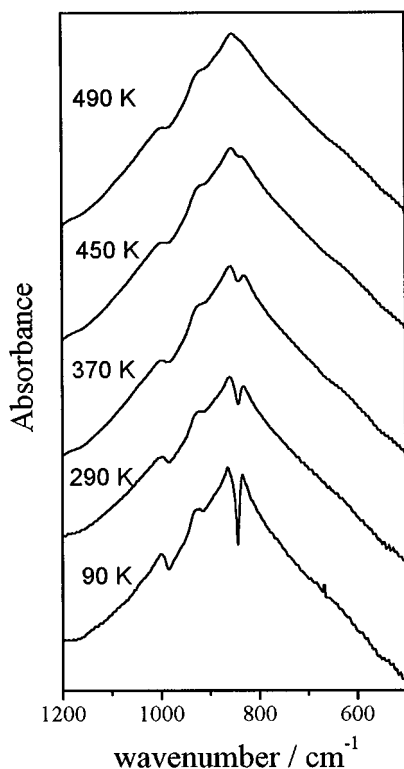


FIG. 3. Polycrystalline temperature dependent IR spectra of the trigonal  $\text{KIn}(\text{WO}_4)_2$  in the stretching modes region.

soft modes. This, however, does not necessary mean that such modes are not present, but may be due to experimental difficulties. Due to very small thickness of crystals, the Raman signal is very weak, especially at elevated temperatures, resulting in difficulties in locating very weak lattice modes.

When temperature is lowered, the splitting of the 801 and 338  $\text{cm}^{-1}$  Raman-active and 992, 914, 851, and 333  $\text{cm}^{-1}$  IR-active internal bands is observed (see Fig. 4 and Table 4). This behavior is very similar to that of  $\text{KSc}(\text{WO}_4)_2$ ; i.e., a very clear splitting is observed for the doubly degenerate components of the  $\nu_3$  and  $\nu_2$  modes, whereas no splitting could be noticed for the  $\nu_4$  mode. As for  $\text{KSc}(\text{WO}_4)_2$ , a large shift with temperature is observed for the bending mode observed at 353  $\text{cm}^{-1}$  at 490 K and 371  $\text{cm}^{-1}$  at 100 K. We have decided to analyze the observed splitting as a function of temperature because many previous studies showed that splitting provides a convenient measurement of the temperature dependence of the order parameter (19). Because the splitting is most clearly observed for the  $E_g$  asymmetric stretching mode at 801  $\text{cm}^{-1}$ , we have fitted the data for this mode. The results are shown on Fig. 5, where the full line is obtained from the fitting of the splitting  $\delta\tilde{\nu}$  to the expression  $\delta\tilde{\nu} = A(T_1 - T)^\beta$ . The obtained parameters are  $A = 6.41 \pm 0.03$ ,  $\beta = 0.24 \pm 0.02$ , and  $T_1 = 475 \pm 16$  K. As one can notice, the obtained transition temperature (475 K)

is significantly higher from that reported in literature (454 K (3)). IR measurements are consistent with the Raman study since they show the presence of a clear splitting at 450 K which disappears above 470 K (see Fig. 3). This disagreement in the phase transition temperature obtained previously and in the present study indicates that this temperature is sample dependent. Such explanation is likely since the crystals are obtained by quenching from a high temperature and therefore a large number of defects is expected to be produced in the sample. The temperature dependence of the splitting is stronger in the case of  $\text{KIn}(\text{WO}_4)_2$  in comparison with that found for  $\text{KSc}(\text{WO}_4)_2$ . For example, 200 K below the transition temperature the splitting is 23  $\text{cm}^{-1}$  for  $\text{KIn}(\text{WO}_4)_2$  and 11  $\text{cm}^{-1}$  for  $\text{KSc}(\text{WO}_4)_2$ . The splitting is the measure of distortion of the crystal structure from the trigonal symmetry and, therefore, such a result indicates that this distortion is stronger for  $\text{KIn}(\text{WO}_4)_2$ . Since according to the theory developed by Otko *et al.* (3) distortion from the trigonal structure is caused by the shift of  $\text{K}^+$  ions from their positions at  $D_{3d}$  sites and rotation of  $\text{WO}_4^{2-}$  tetrahedra, the stronger splitting for  $\text{KIn}(\text{WO}_4)_2$  when compared to that found for  $\text{KSc}(\text{WO}_4)_2$  means that larger shift of  $\text{K}^+$  ions and larger rotation of  $\text{WO}_4^{2-}$  tetrahedra occur for the former compound. The parameter  $\beta$  ( $0.24 \pm 0.02$ ) is smaller than that obtained for  $\text{KSc}(\text{WO}_4)_2$  ( $0.33 \pm 0.01$ ). If we could apply the relations found by Petzelt *et al.* (19), the observed splitting should give information about temperature dependence of the order parameter because the splitting of a hard mode is usually proportional to the order parameter or square of the order parameter. In the former case we could expect that  $\delta\tilde{\nu} \sim \eta \sim (T_1 - T)^{0.24}$  and in the latter that  $\delta\tilde{\nu} \sim \eta^2 \sim (T_1 - T)^{0.24}$ . The first case seems to be reasonable but because of the problems in establishing the temperature dependence of soft modes (see discussion below) we could not give any evidence that it is correct. The previous study of  $\text{KSc}(\text{WO}_4)_2$ , for which both the data on splitting and temperature dependence of soft modes are available, suggests, however, that the relation between the splitting and the order parameter is not as simple as derived by Petzelt *et al.* (19) by taking into account the lowest coupling terms only. In other words, in order to explain properly the relation between the order parameter and the observed splitting, the higher-order coupling terms should be taken into account. It is, therefore, very likely that the temperature dependence of the order parameter is the same as that found for  $\text{KSc}(\text{WO}_4)_2$  (15) and  $\text{KSc}(\text{MoO}_4)_2$  (3) and predicted by Otko *et al.* (3); i.e.,  $\eta \sim (T_1 - T)^{0.5}$ , not  $\eta \sim (T_1 - T)^{0.24}$ .

At 100 K six Raman-active modes are observed in the lattice modes region. The highest frequency 152  $\text{cm}^{-1}$  band can be assigned to the two overlapping  $T'(\text{WO}_4)$  modes described above. These modes are not separated even at 100 K. This behavior is different from that of  $\text{KSc}(\text{WO}_4)_2$ ,

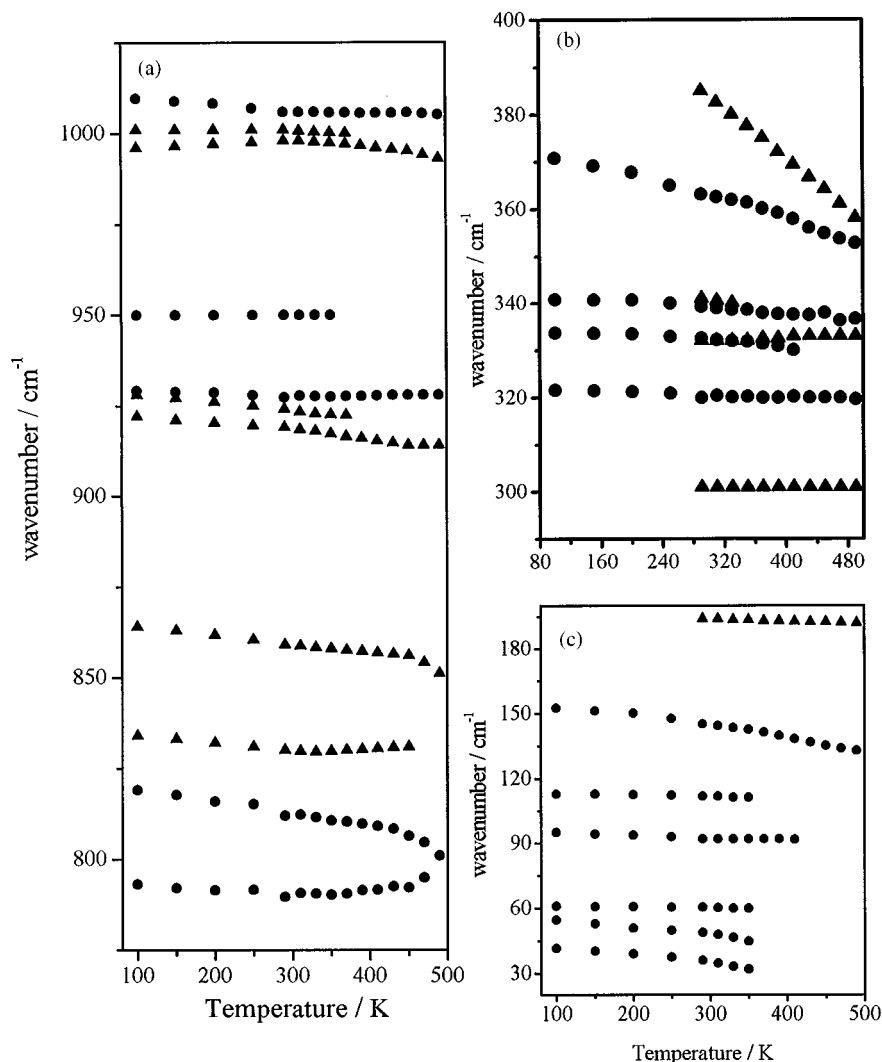


FIG. 4. Raman (closed circles) and IR active modes (triangle) vs temperature for the trigonal  $\text{KIn}(\text{WO}_4)_2$ : (a) stretching modes; (b) bending modes; and (c) lattice modes.

where two clear bands were observed at 147 and  $136\text{ cm}^{-1}$  (15). It is worth noticing that the band width of the  $T'(\text{WO}_4)$  mode ( $10.0\text{ cm}^{-1}$  at 100 K) is significantly higher than the values found for  $\text{KSc}(\text{WO}_4)_2$  ( $5.4$  and  $6.5\text{ cm}^{-1}$  for the  $147$  and  $136\text{ cm}^{-1}$  components, respectively). Such a result supports the conclusion that this band is composed of two overlapping bands of similar energy. As for  $\text{KSc}(\text{WO}_4)_2$ , the  $T'(\text{WO}_4)$  modes exhibit pronounced broadening with increasing temperature, indicating the presence of some kind of disordering at high temperatures. The doubly degenerate librational mode can be easily located at  $62\text{ cm}^{-1}$  since the previous study of a number of molybdates and tungstates located this mode in a narrow frequency range,  $45\text{--}64\text{ cm}^{-1}$  (15,20). This mode is very weak and we could not observe any increase in its intensity with heating. This behavior is very similar to that of  $\text{KSc}(\text{WO}_4)_2$  where this mode was

shown to be relatively strong only after prolonged keeping of the crystal at temperatures above  $T_1$ .

The  $93\text{ cm}^{-1}$  band can be most likely assigned to the nondegenerate librational mode, observed at  $103\text{ cm}^{-1}$  in  $\text{KSc}(\text{WO}_4)_2$ . It is worth noticing that its intensity is a few times higher than the intensity of the doubly degenerate librational mode. The same behavior was observed for  $\text{KSc}(\text{WO}_4)_2$ . In case of  $\text{KIn}(\text{WO}_4)_2$  we observe one additional band in comparison with  $\text{KSc}(\text{WO}_4)_2$ . This  $112\text{ cm}^{-1}$  band is assigned to the  $T'(\text{K}^+)$  mode and it was not observed for  $\text{KSc}(\text{WO}_4)_2$ , probably due to accidental degeneracy with the librational mode.

The remaining lattice modes at  $54$  and  $41\text{ cm}^{-1}$  (at 100 K) can be most likely attributed to the soft modes since they show clear softening with increasing temperature (see Fig. 4). Unfortunately, we could not establish the

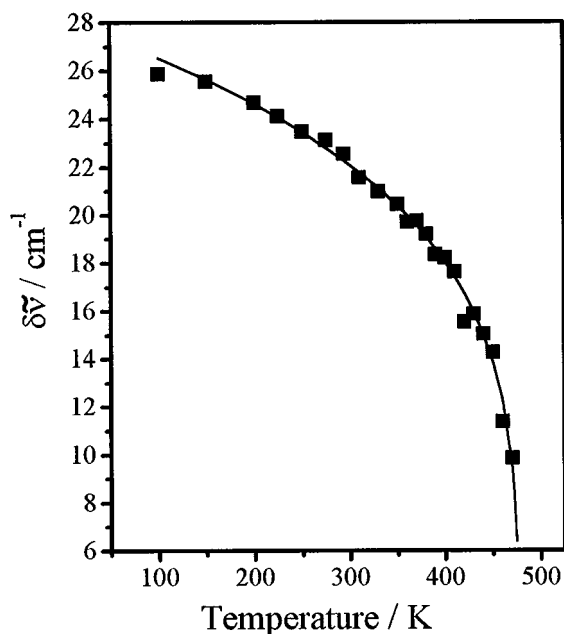


FIG. 5. Frequency splitting ( $\delta\tilde{\nu}$ ) of the asymmetric stretching mode as a function of temperature. Solid line has been obtained from the fitting of  $\tilde{\nu}$  to the expression  $\delta\tilde{\nu} = A(T_1 - T)^\beta$ .

temperature dependence of these modes due to the lack of data above 350 K. This lack of data is due to experimental difficulties. As mentioned above in order to avoid transformation of the crystals into the orthorhombic phase, the trigonal crystals can be grown only with a fast cooling rate (see Experimental). As a result, crystals grow as large but very thin plates. Therefore, measurements are possible only in backscattering configuration and the signal is weak. In spite of the experimental difficulties in measuring the scattered light from thin crystals, the internal and some lattice modes can be well observed since these phonons are good scatters. However, the modes below  $100\text{ cm}^{-1}$  are very weak, their intensity and frequency decreases with increasing temperature and band width increases, leading to very serious problems in locating these modes above 350 K.

### CONCLUSIONS

The results of IR and Raman investigations of the low- and high-temperature phases of  $\text{KIn}(\text{WO}_4)_2$  have been presented for the first time. The assignment of observed bands has been proposed. The present results are consistent with the X-ray investigation showing that the orthorhombic phase of  $\text{KIn}(\text{WO}_4)_2$  is isomorphic to the orthorhombic structure of  $\text{RbIn}(\text{MoO}_4)_2$ . The measured spectra show high degree of coupling among vibrational modes.

The temperature behavior of the trigonal phase of  $\text{KIn}(\text{WO}_4)_2$  is very similar to that observed for  $\text{KSc}(\text{WO}_4)_2$

although the X-ray study suggests that the both crystals differ in respect to space groups. The two compounds differ only in the following details:

— The splitting of the  $\nu_3$  mode at  $801\text{ cm}^{-1}$  is larger for  $\text{KIn}(\text{WO}_4)_2$  when compared to that found for  $\text{KSc}(\text{WO}_4)_2$ , indicating stronger distortion from the trigonal symmetry in the former crystal.

— The temperature dependence of this splitting is different for the both crystals; i.e.,  $\delta\tilde{\nu}$  is proportional to  $(T_1 - T)^{0.33}$  for  $\text{KSc}(\text{WO}_4)_2$  and  $(T_1 - T)^{0.24}$  for  $\text{KIn}(\text{WO}_4)_2$ .

— No separation of the two  $T'(\text{WO}_4)$  modes at 100 K is observed for  $\text{KIn}(\text{WO}_4)_2$  whereas it is observed for  $\text{KSc}(\text{WO}_4)_2$ . This is due most likely to accidental degeneracy.

—  $T'(\text{K}^+)$  mode is clearly observed for  $\text{KIn}(\text{WO}_4)_2$  although it couldn't be observed for the scandium derivative. Finally, we conclude that the present results do not provide any evidence that the high-temperature crystal structure of  $\text{KIn}(\text{WO}_4)_2$  is described by the space group  $D_{3d}^4$  instead of the  $D_{3d}^3$  one. The properties and phase transition mechanism seems to be nearly the same for both  $\text{KSc}(\text{WO}_4)_2$  and  $\text{KIn}(\text{WO}_4)_2$ , and they agree well with the theoretical predictions made for the space group  $D_{3d}^3$ .

### ACKNOWLEDGMENT

This work was partially supported by the Polish State Committee for Scientific Research, Grant 3 TO9B 090 15, and the Foundation for Advancement of International Science. M.M. acknowledges the Japan society for the Promotion of Science for the financial support of his stay at the University of Tsukuba, where the temperature-dependent Raman spectra were measured.

### REFERENCES

1. G. E. Peterson and P. M. Bridenbaugh, *Appl. Phys. Lett.* **4**, 173 (1964).
2. A. A. Kaminskii, A. Kholov, P. V. Klevtsov, and S. Kh. Khafizov, *Phys. Status Solidi A* **114**, 713 (1989).
3. A. I. Otko, N. M. Nesterenko, and L. V. Povstyanyi, *Phys. Stat. Solidi A* **46**, 577 (1978).
4. A. I. Otko, N. M. Nesterenko, and A. I. Zvyagin, *Izv. Akad. Nauk SSSR, Ser. Fiz.* **43**, 1675 (1979).
5. N. M. Nesterenko, V. I. Fomin, and V. I. Kutko, *Fiz. Nizk. Temp.* **8**, 86 (1982).
6. W. Zapart, *Phys. Status Solidi A* **118**, 447 (1990).
7. W. Zapart and M. B. Zapart, *Phys. Status Solidi A* **121**, K43 (1990).
8. M. B. Zapart and W. Zapart, *Phase Transitions* **43**, 173 (1993).
9. V. A. Efremov, V. K. Trunov, and Yu. A. Velikodnyi, *Sov. Phys. Crystallogr.* **17**, 1005 (1973).
10. M. Mączka, *J. Raman Spectrosc.* **30**, 971 (1999).
11. P. V. Klevtsov, L. P. Kozeeva, and L. Yu. Kharchenko, *Sov. Phys. Crystallogr.* **20**, 732 (1975).
12. P. V. Klevtsov, R. F. Klevtsova, and A. V. Demenev, *Kristallografiya* **17**, 545 (1972).
13. M. Daturi, G. Busca, m. M. Borel, A. Leclaire, and P. Piaggio, *J. Phys. Chem. B* **101**, 4358 (1997).



14. L. Yu. Kharchenko and P. V. Klevtsov, *Zh. Neorg. Khim.* **21**, 2836 (1976).
15. M. Mączka, S. Kojima, and J. Hanuza, *J. Phys. Soc. Jpn.* **68**, 1948 (1999).
16. M. Mączka, S. Kojima, and J. Hanuza, *J. Raman Spectrosc.* **30**, 339 (1999).
17. M. Mączka, J. Hanuza, E. T. G. Lutz, and J. H. van der Maas, *J. Sol. State Chem.* **145**, 752 (1999).
18. M. Mączka, *Eur. J. Solid State Inorg. Chem.* **33**, 783 (1996).
19. J. Petzelt and V. Dvorak, *J. Phys. C* **9**, 1571 (1976); *ibid.* 1587.
20. M. Mączka, S. Kojima, and J. Hanuza, *J. Kor. Phys. Soc.* **35**, S1503 (1999).